APEM journal
Advances in Production Engineering & Management **ISSN 1854-6250**
Volume 8 | Number 2 | June 2013 | pp 96–106 Journal home: apem-journal.org
http://dx.doi.org/10.14743/apem2013.2.157

Additive manufacturing of biocompatible ceramics

Goffard, R.[a,*], **Sforza, T.**[b], **Clarinval, A.**[b], **Dormal, T.**[b], **Boilet, L.**[c], **Hocquet, S.**[c], **Cambier, F.**[c]

[a]CRIG, Centre de Recherche des Instituts Groupés, 27 Quai du Condroz, 4030 Angleur, Belgium
[b]Sirris, Additive Manufacturing Department, 12 Rue du Bois Saint-Jean, 4102 Seraing, Belgium
[c]BCRC, Belgian Ceramic Research Center, 4 Avenue Gouveneur Cornez, 7000 Mons, Belgium

ABSTRACT

Considering that the ageing of the population is not going to stop, the need for biocompatible materials is continuously increasing, especially in the field of bone substitutes as well as in the fabrication of surgery tools. The Optoform process is an additive manufacturing technology able to shape most of the common biocompatible ceramic materials such as hydroxyapatite (HA) and tricalcium phosphate (TCP). Those ceramic materials are largely studied to substitute bone defects or as voids fillers while stronger bioinert materials like alumina and zirconia can find applications in surgery tools or in dentistry. The Optoform process allows building a component, layer by layer, from CAD data, leading to significant advantages: 1) the manufacturing of elements with a complex geometry and with a controlled porosity that would be impossible to demold or to machine; and 2) short delays of production for customized part with the desired characteristics and design. The quality control of these parts is essential for medical use and is certified by the control of each step of the manufacturing process: synthesis of biocompatible ceramic powders, preparation of photo-curable resin based paste, shaping of the part by Optoform and subsequent thermal treatment for debinding and sintering.

© 2013 PEI, University of Maribor. All rights reserved.

ARTICLE INFO

Keywords:
Biomaterial
Ceramic
Rapid manufacturing

**Corresponding author:*
raphael.goffard@sirris.be
(Goffard, R.)

1. Introduction

1.1 Bone defects and implants

Traumas, tumours, infections, accidents, congenital malformations are many causes that might lead to bone defects. When the bone missing part has a critical size, the body cannot heal it by itself and the defect needs addition of bone graft material in order to fill the void. Surgeons can then consider many options such as autograft, allograft, or the use of synthetic materials [1]. Autologus materials can be considered as a paragon of excellence but they present several problems such as a limited availability and the necessity of several surgical incisions. Allografts, on their side, might lead to diseases transfer or tissue refusals. Alloplastics are not harvested from donors, neither from another place in the body and thus those risks are highly reduced and there is no availability limits.

Nowadays, many different materials are available for alloplastic bone replacement surgery such as titanium, polymers and ceramics. They have diverse properties fitting for various applications. Some of them are only biocompatible and stay inert in the body (such as alumina or zirconia), performing a mechanical reinforcement or protecting a vulnerable structure. Others are bioactive: a biological link is created with the material, facilitating the incorporation of the im-

plant and the stresses transmission (like HA). Finally, others are absorbable and thus tend to be replaced by surrounding ingrowing bones (for example the β-TCP) [2].

1.2 Additive manufacturing of ceramics

The most common techniques to shape ceramics are tooling and moulding but it is also possible to use an additive technology such as 3D printing or stereolithography.

Additive techniques offer the advantages to produce quickly customized part directly from CAD data. Such customized implant can have very complex geometries with, possibly, interconnected porosity, without causing any additional difficulties to the production. Medical imagery can give information essential for the design of a tailored implant for a specific bone defect. 3D printing of implants or scaffolds using calcium phosphate is already in the focus of scientific researches [1, 3].

Stereolithography of ceramics has also already been experienced [4]. In this study, we are using an OPTOFORM machine. The OPTOFORM was developed in 2000 in order to carry out rapid prototyping with metal, ceramic or any materials. OPTOFORM is then a stereolithography machine especially well designed for experimenting new materials. The study presented below uses UV curable resins filled with ceramic powders. Once the suspension is prepared, it is spread on the working area thin layer after thin layer. The shape and size of the implant are directly transferred from a CAD file to the stereolithography machine where a UV laser beam polymerizes the resin layer after layer. Once the production is achieved, a thermal cycle is performed in order to pyrolyse all the organics components (the resin) and to sinter the ceramic. Indeed, if organics are still present in the final product, the physical properties and the biocompatibility will be altered.

Additive manufacturing offers a total freedom in the design of the manufactured parts. The implants may have an integrated structure of interconnected pores that would promote cells adhesion and facilitate subsequent bone ingrowth [5]. The porous structure (level of porosity, size, shapes and interconnectivity of the pores) has shown to have a net influence on the bone regeneration in the implants [6, 7].

The aim of this study is to master every step of OPTOFORM manufacturing process and to assess its dimensional accuracy. As the quality control of the produced parts is essential for its clinical use, it is also very important to be aware of the mechanical and physical characteristics of the productions.

2. Materials and methods

2.1 Optoform machine, data acquisition, CAD of the parts

The Optoform (Fig. 1) is an experimental stereolithography machine. Starting from a 3D STL file, a part is built slice by slice from bottom to top, on a plate recovered with a polymer paste which hardens when scanned by a UV laser beam [8].

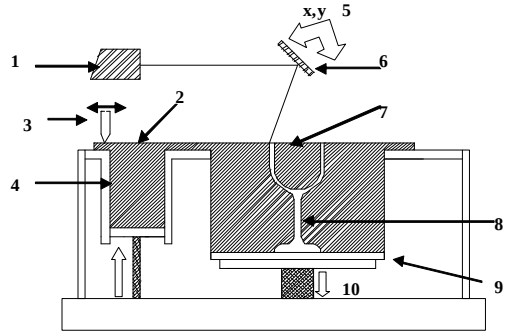

Fig. 1 Optoform principle: 1: UV Laser, 2: paste supply, 3: recoater including a blade and 2 rotating rods, 4: paste tank, 5: XY rotation, 6: galvanometrical mirror, 7: photosensitive paste, 8: polymerised prototype, 9: building platform, 10: z control

Depending on the geometry of the part and on the material, the building speed is around 375 cm^3/h and up to 750 cm^3/h and there is no waiting time during the recoating. Unlike usual stereolithography, the UV scanning is immediate after the passage of the blade [9].

Supports are needed because of the scraper stress. The layer thickness is a function of the material reactivity to UV and of the application, but it is always in the range of 35–120 μm. The maximum size of the prototype is 250 mm × 350 mm × 500 mm but there are also smaller platforms more suitable to process expensive material or to build small implants. Actually, no ceramic parts of the size of the biggest platform have ever been produced because of ceramic brittleness.

The STL file of the part can be obtained through different ways depending on what is to produce. Surgical tool parts or any mechanical component are obtained via CAD while cranial flap or other biological volumes are often the result of a medical imagery. The patient's skull is scanned and the virtual generation of the implant is obtained by performing a mirror function of the healthy part of the skull [1]. Implants can be designed with CAD software if their geometry is not too complex and/or if their size is to be standardized.

Once a computer file of cranial flap is available a porous structure can be synthesizes on its contours to promote bone regeneration around and inside the implant. The porous structure is created with "SolidWorks" (© Dassault Systems 1995–2012) and is then subtracted from the implant file with the software "Magics" by Materialise.

To avoid having marks from the supports on the part an "under-part" is created. Using Magics again, the lower surface of the implant is copied and extruded on a very thin thickness. This newly created volume consists of the under-part. It is positioned fractions of millimeter below the implant having no contact with it. The supports will hold the under-part in place on the building platform. During the fabrication, the implant and the under-part are interdependent thanks to the surface tension induced by the non-polymerized paste that is spread between the two parts.

The STL files of the supports and the implant are then transferred in "Optovue" (© OptoForm 1997–2001), a slicing software dedicated to Optoform. Slices of the desired thickness are then created representing sections of the implant. The laser tracks are also defined at this point. The file containing the sliced volume is introduced in "Optobuild" (© OptoForm 1997–2001), the machine program and the fabrication can be launched.

2.2 Optoform machine, data acquisition, CAD of the parts

Every material developed for the Optoform machine must comply with specific criteria. Each material includes some resin, fillers (from 20 % up to 70 % in volume) and a photo-initiator [10, 11]. In addition, it could contain rheological agent, thixotropic additives and wetting agent. The ceramics used for the OptoForm are bought to Valutec SA (Valenciennes, France). HA and β-TCP powders are prepared by the aqueous precipitation technique, using diammonium phosphate solution $(NH_4)_2HPO_4$ and calcium nitrate solution $Ca(NO_3)_2\ 4H_2O$. Temperature and pH are adjusted depending on what is to produce, HA or β-TCP powder. After filtering the solution and drying the precipitate at 70 °C, the powders exhibit a very high specific surface area (> 60 m^2/g), that does not permit to obtain good paste for OptoForm process. Particle size of β-TCP and HA precipitates are increased by a thermal treatment at an adapted calcinations temperature in order to obtain the desired grain size. After this step, powders are ground to break up agglomerates formed during calcinations and to reduce the powder to its ultimate particle size [12].

The paste must have the firmness of toothpaste which does not flow with the gravity. The viscosity and the flow behaviour can be interpreted with the Bingham's model. Thanks to the paste consistency, no tank is needed to build a model.

The mixture has to be stable in time and the filler should not deposit sediment. Basic curing resins of those materials are generally acrylates, methacrylates or epoxy [10, 11].
In any case, after building, the parts require a cleaning step. This task issue will be undertaken by a wise choice of solvent, which will dissolve the paste and not the part.

2.3 Ceramics

In this project, the paste filler is always a biocompatible ceramic. Several pastes with different ceramics have been developed to offer various characteristics intrinsic to each material and providing solution to different needs. The ceramics paste developed here are HA, β-TCP, alumina, and more recently a mixture of HA/β-TCP and zirconia. HA, hydroxyapatite is a bioactive material promoting bone ingrowth, offering a good resistance in compression and with a very slow rate of bioabsorption. It is suitable for long term implantation. β-TCP, beta tricalcium phosphate is a biocompatible ceramic that can be resorbed within a few weeks in the body for the smaller parts, it also promotes bone ingrowth very efficiently. Alumina is a biocompatible material with really strong mechanical properties but no bioactivity has ever been reported. HA/β-TCP is a mixture of two different ceramic powders. The purpose of this biphasic compound is to adapt bioresorption rates to the speed of bone ingrowth. Zirconia is known for its particularly high mechanical resistances as well as a good tenacity and wear resistance in comparison with other bioceramics.

2.4 Production

Important parameters of scaffolds and implants for bone replacement are the compression strength and the Young modulus of the material [13]. HA samples have been produced in order to receive 3 points bending tests, compressive tests, and densification rates tests. For all developed materials, parts 15 mm thick without porosity were produced in order to check the ability to debind and sinter parts of different size and thickness. Implant parts of various geometries of small and large dimension were produced with high, low and evolving porosity degree to make sure the machine parameter are versatile enough to produce any kind of geometry. To observe the minimal pore size achievable by the Optoform we produced parts with various pore dimensions from 0.7 mm to 0.3 mm. Prototypes of cranial flap implant and tibial osteotomy wedge (with an external ring dense and the inner part imitating cancellous bone) have been manufactured among others in HA and in HA/β-TCP.

Some geometry and dimensional tests were performed on the most complex shapes in order to verify the accuracy of the process.

2.5 Debinding and Sintering

Debinding and sintering cycle is one of the key steps of this entire process. Pyrolysis is very important as it removes organics from the green preceramic and makes it a pure biocompatible ceramic.

These cycles were defined at the BCRC following weight loss (TGA) during the pyrolysis of organics. The cycles are performed under air. The sintering part of the cycle occurs at higher temperature but always below melting point [14]. During sintering, ions and atoms move and fill up open channels between the grains of ceramic powder (organics evacuation leaves a lot of voids in the parts), Fig. 2.

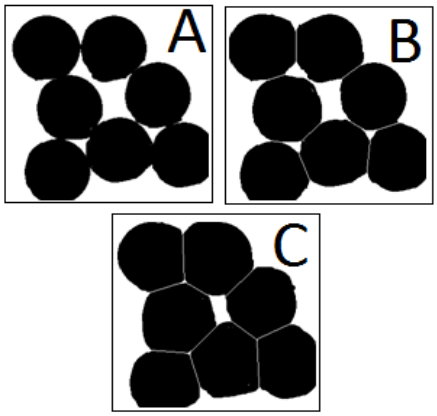

Fig. 2 Different steps (A, B & C) of sintering process, the grains are filling up the void channels left by the debinding

This mechanism comes with a high degree of shrinkage but in general the shape is conserved. This shrinkage gives the piece its density and so its mechanical properties. The sintering temperatures depend on the studied ceramic material while heating rates, dwell temperature and holding times depend on the organics used in the paste.

2.6 Mechanical and dimensional characteristics

Different tests were performed in order to evaluate the quality of the manufactured parts. As mentioned in subsection 2.4, we have performed various mechanical tests on HA while other material except from zirconia (which is too recent) have only received dimensional and density tests. HA is the only material that has been mechanically characterised because in term of density it is the most accomplished with the alumina. Density is a key parameter in the physical and mechanical properties and thus it has been calculated for every used material but zirconia. Densification rates have been calculated with the Archimedes' principle. Accuracy of the process have been evaluated and improved with by different means: visual checking, microscope and 3D scan.

2.7 Biocompatibility

Beside mechanical and dimensional characteristics, an implantable object must comply with a biological environment. Porous sample of β-TCP were then tested in a human cell culture in order to evaluate the cells reproduction around the specimen. Other samples have been screwed into the backbones of several rats in order to assess the biodegradation of the implant as well as the bone ingrowth in the implants.

3. Results

3.1 Production

The CAD/CAM of the implants, tools elements and test parts went well. Delaminating systematically occurred between two layers on parts containing too many slices.

A paste with correct consistency has been found for every material. All the selected pastes spread correctly on the working platform without generating any difficulties and they all had the required viscosity to be able to build parts tall enough without observing any collapsing of the paste heap.

3.2 Debinding and sintering

Difficulties were met during the debinding cycles: cracks appeared when pyrolysis occurred too fast and the organics did not have the time to evacuate the green preceramic slowly. This problem was solved by adjusting the temperature rising rate. Using TGA, the most appropriate cycles have been found. As similar resins are used in every paste, the cycle always consists of three dwell steps at 180 °C, 400 °C and 430 °C plus a sintering period at a temperature depending on the material.

Between debinding and sintering, parts are very weak. As an example, the cranial flaps collapsed (Fig. 3) during thermal cycle when not correctly supported due to their shape (a large proportion of the piece is in cantilever and needs to be supported).

For every paste composition the degrees of shrinkage were different. Also, shrinkage is always most significant in the vertical direction. Such a phenomenon is taken into account while designing the parts that are to be manufactured [15].

Not only the sintering is critical; the burning of the organics occurring during debinding is very sensitive; especially with HA/β-TCP specimens. If using the same speed with this material than with others, cracks can appear at only 90 °C.

Fig. 4 shows microscopic views of β-TCP samples after a thermal cycle. It can be observed that after the first part of the cycle (until 600 °C) all the organics are gone away and the ceramic grains are easily identified, Fig. 4 (left). Fig. 4 (right) is the image of a similar sample after completing sintering cycle. A large grain growth occurs during the thermal treatment.

Fig. 3 The cranial flap collapsed when having a thermal cycle because it was too weak to carry its cantilever parts between debinding and sintering

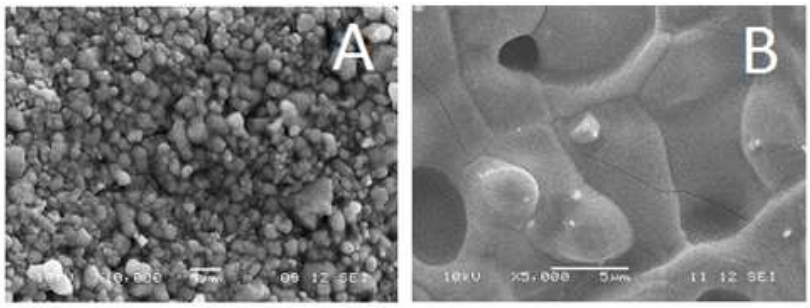

Fig. 4 SEM analysis of β-TCP samples after pyrolysis of the resins (left) – (×10000) and after sintering of the ceramic grains at 1130 °C (right) – (×5000)

3.3 Mechanical and physical properties

Density is a very easy property to measure and it gives good indication about the sample's possible mechanical resistances. This is why density measurement is the first test carried out on samples. Table 1 shows densities as we can reach them now with the selected production paste, parameter and thermal cycle.

Compression tests have been performed on different types of samples (Table 2) in order to better understand the limitation of the process. Those characteristics have not been measured with the best process parameters, as at the time the tests were made, research for the optimised production parameters was still going on. Higher strengths have been reached by now. But those tests permit to highlight some characteristics inherent to the process.

Table 1 Average relative densities of the developed materials

Material	Relative density (%)
Alumina	92
HA	95
β-TCP	88
HA/β-TCP	79

Table 2 Compression strength of HA cubes with different characteristics. The process parameters were different for the pore shape tests and for the directional compression tests. So the compression strength values in itself are not meaningful, only the comparison of two results of the same test has a meaning.

Type of sample	Compression strength (MPa)
60 % macroporous cube (square pores)	9.4 ± 1.7
60 % macroporous cubes (round pores)	20.8 ± 0.7
Compression direction ⊥ to the layers on full cubes	9.4 ± 0.8
Compression direction // to the layers on full cubes	20.7 ± 5.0

Table 3 Compressive and bending strength of HA samples

Compressive strength (// to the layers)	111 MPa
Bending strength (3 points bending test)	26.1 MPa

HA is the material that has been the most characterised among the materials developed for this project. HA is widely used as bone replacement so it was important to have it characterised. Table 3 shows the best values obtained as we can reach them now with the optimised process parameters.

3.4 Dimensional analysis and geometries

The physical characteristics of produced materials are crucial in order to evaluate the potential medical use of the products but it is certainly not the only thing to take into consideration. The respect of the shapes and dimensions are also very important, especially when considering patient tailored implants. There is no point in tailoring an implant if the accuracy of the process is not sufficient. In this study we checked the accuracy of several cranial flap prototypes by three means:

- Placing the flap on the skull corresponding to the studied bone defect and evaluating the harmony of the two parts (Fig. 5).
- Performing a 3 dimensional scan of the produced flap and comparing it with the original CAD file (Fig. 6). Scanning was performed with a structured-light 3D scanner Atos while the dimensional analysis was done using the software GomInspect software (© Gom 2012). We observed a difference of 0.2 mm on big parts such as skull implant (not represented on the picture)
- Looking at a porous sample through a microscope with low power magnifier and measure the size of the pores (Fig. 7). A pore dimension of 0.7 mm with an in-between section of 0.4 mm was expected. Fig. 7 shows the parts before sintering so 1.25 times bigger than the finished product. The accuracy is quite good.

Fig. 5 Hydroxyapatite flap implant fitting in the reconstitution of a skull with a defect

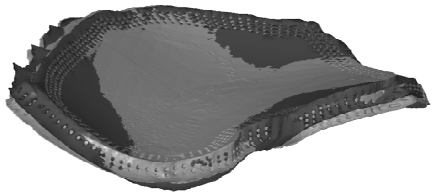

Fig. 6 Print screen from GomInspect with the original STL file of a cranial flap (coming from medical imagery) in dark colour superposed with the STL of the scanning of the produced flap. For better visualization, the example here shows parts that are not well superimposed.

Accuracy is also very important for the mechanical parts. The accuracy reached with alumina permit us to screw the manufactured part on the fillet of a surgical tool. This dimensional mastering was achieved despite the high shrinkage occurring during the thermal cycles.

The porous structure integrated to the implants with Magics permitted us to manufacture implants with interconnected pores and controlled porosity.

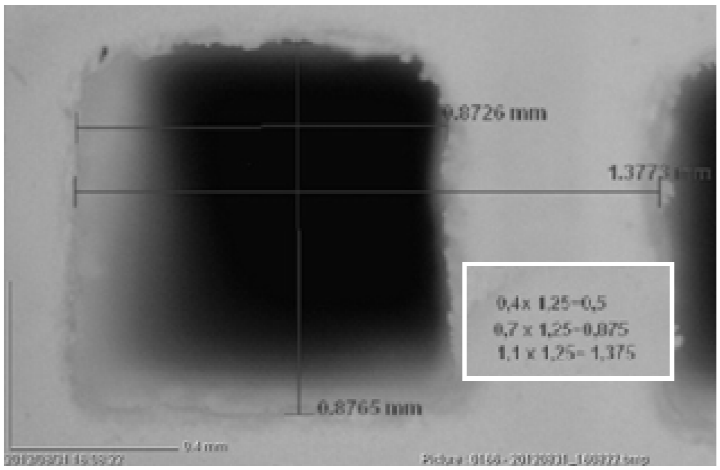

Fig. 7 Microscography of a pore on a porous sample we can see that the pore dimension are 0.8765 and 0.8726 ≈ 0.875 = 1.25 mm × 0.7 mm and that the distance between two pores is 1.3773 ≈ 1.375 = (0.4 + 0.7) mm × 1.25 mm

Specimens presenting different pore sizes were built with the purpose to determine the smallest pore size that can be made and cleaned from the post fabrication paste only by blowing air. In fact, the smallest pore size is the same for all tested materials (as it is determined by the laser beam accuracy and the building parameters) but some of them are more difficult to clean due to the rheological behaviour of the paste that is different from one material to another. The viscosity changes because the resin mixes are different as well as the specific surface area of the ceramic powder.

A simulation of fluid flow through different architectures of interconnected pores (with 1, 4, 8 and 12 faces pores) showed us a variation of only 0.7 % of the biological fluid flow through the structure.

The customized character of the implants is well realized. No difficulty is encountered when meeting any special geometry to produce. It asks no longer time to build 20 different implants for 20 different people than to produce 20 times a standardized implant. We can process in the same production a flap implant and porous scaffolds without any difficulty. As long as the work is done in medical imagery, any medical implant or device can be produced as fast and easily as a simple cube (considering elements of the same size of course).

3.5 Biocompatibility

The human cell culture showed encouraging results, the amount of cells has been multiplied by 4 in 13 days around the β-TCP samples.

Samples of β-TCP implanted in the rats have shown a good rate of biodegradation as well as a good bone invasion. This bioactive behaviour of the β-TCP has already been confirmed in the literature [16].

4. Discussion

Optoform stereolithography of ceramics enables the production of unique and very complex volume and structure such as tailored implants or scaffolds for bone reconstruction or a mix of both: an implant with an integrated scaffold with controlled architecture and porosity.

Biocompatible ceramics rapid manufacturing technologies offer to the surgeon a good alternative to the calcium phosphate or acrylic bone cements that are currently used. These cements are often unable to fulfil the aesthetic requirements because of the dexterity it asks to surgeon to modify and shape the implant during the operation. Moreover, it has been shown that the exothermic curing reaction of acrylic cement can be at the origin of tissue inflammations, infections, necrosis or even rejections of the implants [17]. The use of prefabricated implant diminishes the operation time and thus the risk of complications. It also gives more guarantees on the aesthetic result.

4.1 Geometry

Integrated porous structure is a great plus on a bone implant. A recurrent problem with implant is the appearance of necrotic tissues on the centre of the scaffold due to the limited penetration of cells and nutriment in the implant [7]. When macro pores are interconnected, nutriments and cells migration into the centre of the implant is privileged.

Given the very small differences of fluid flow through the different pore geometries we should generally choose a circular geometry because, as mentioned in Table 3 as there is less stresses concentration, the compression strength is higher.

The dimensional accuracy (± 0.2 mm) is suitable for operatory guides, for most of the tools and for implants. Thanks to an operation guide a surgeon can operate a dissection or mill a hole in the patient bone at a desired position. With 0.2 mm of accuracy on the guide, a good positioning is obtained.

This accuracy is also enough for many mechanical parts as it allows the screwing of the ceramic part on the fillet of a metallic tool.

Fig. 5 shows that fitting a flap on the cranial defect is almost perfect with such accuracy.

4.2 Properties

The density of a ceramic is the result of its sintering. It has to be noticed that densification rate is largely dependent on the grain size of the initial powder. Smaller is the powder easier is the sintering [18]. In our case, we are unable to use very thin powder because of the dependence of the paste viscosity. Indeed, too thin powders also lead to a very viscous paste that would not be spreadable on the working platform.

In our case of porous implants, it is very important to reach a high density in order to ensure sufficient mechanical resistance despite the high level of "macro" porosity.

The values obtained by stereolithography process in terms of compression and bending strengths are encouraging by comparison to values obtained by the 3D printing process of calcium phosphate. The bending strength reached is between 3.9 MPa and 5.3 MPa [1] on dense samples against 26.1 MPa in Table 3. Under compression, 3D printed samples do not have higher strength than 21.2 MPa [12] while sample in this study reached 111 MPa. The good densification rate reached explains in itself the better mechanical characteristics. Densification rates obtained by 3D printing are around 65 % [1].

Mechanical properties are encouraging compare to other processes of additive manufacturing of ceramic but it is still far from the valued obtained with HA sample shaped by moulding and fully densified thanks to a HIP post sintering operation. Those samples had a 105 MPa in bending strength.

HA has been developed with the purpose to be used as bone replacement so it is also interesting to compare the strength the optoformed samples with strength of bone. According to literature tibia has an average compressive strength between 120 MPa and 150 MPa [19]. Those are average values and they have to be watched carefully as bone quality changes a lot from one individual to another.

Results of Table 2 regarding the strength variation in function of the direction of compression may be explained by a lower density on the surface between each layer so when compress perpendicularly to those layer a specimen might fail at this interstice while the strength is continuous all along the sample when charge is applied in parallel with the layers.

Anyway densities such as the one reached in alumina and HA would allow a post sintering treatment such as HIP and thus give better densities and higher mechanical strength.

4.3 Application

Depending on the ceramic used we can reach many diverse activity fields with this technology.

The β-TCP offers application in bone scaffolds and temporary implants. Bone substitutes made of this material are highly biodegradable and thus have to be placed where bones have rapid growing abilities. It must above all be small dimension parts so that a new real bone can rapidly replace the bioresorbed prosthesis.

HA is almost non-resorbable. It has a very low speed of biodegradation and it creates links with the biological surrounding tissues. As it stays in place much longer, this ceramic also offers a better long term resistance to the stress of the body on the implant. Such a material can thus be very suitable for cranial flaps for example. Unfortunately ceramics have low bending resistance and do not offer the possibilities for long bone such as a hip implants.

A mix of HA and β-TCP with each of the material in the appropriate proportion is being developed. This mix would have the feature to absorb at the same speed as the bone growths in the implant allowing to keep constantly a good resistance.

The method proposed in this paper is also very attractive in terms of costs: the fabrication of a cranial flap is about 2 to 3 times cheaper by this method in comparison to the grinding of HA ceramic.

5. Conclusion

We showed in this study that with an appropriate technique, stereolithography of various ceramics is possible and efficient. This technology has a great future in medical applications. In implantology it allows avoiding disadvantages caused by intraoperative manual modelling implant. Despite the lowest strength of the materials compare to the same materials shaped with other technique, it permits to manufacture very complex and unique geometries such as an adapted controlled and variable macro porosity that can serve as bone scaffold. Rapid manufacturing gives a fast and cheap tailored implant with a great accuracy. Mixing of active and absorbable ceramics is possible and would allow adapting the bioresorption rate to the bone ingrowth rate. Because of the need of macroporous geometry for scaffolds, rapid manufacturing will maybe become a golden standard in bone implantology. The success in alumina production have applications in medicine for surgery guide or for tools parts manufacturing but it also opens doors of many other fields of activity. Whenever a unique and or complex geometry is needed in alumina, the stereolithography is a promising solution.

Acknowledgements

We would like to thanks the Walloon region for its financial supports in the project OPTOBIO. In addition we thanks Dr. D. Nimal for the cell culture, the rats implanted and the STL file of a cranial flap. Thanks to Centis, Medsys and Dr ph. Docquier for their case studies and STL files.

References

[1] Klammert, U., Gbureck,U., Vorndran, E., Rödiger, J., Meyer-Marcotty, P., Kübler, A.C. (2010). 3D powder printed calcium phosphate implants for reconstruction of cranial and maxillofacial defects, *Journal of Cranio-Maxillo-Facial Surgery*, Vol. 38, No. 8, 565-570, doi: 10.1016/j.jcms.2010.01.009.

[2] Benaqqa C. (2003). *Etude de la propagation sous critique de fissures dans les phosphates de calcium: cas de l'hydroxyapatite et du phosphate tri-calcique*, Unpublished doctoral dissertation, University of Lyon, Lyon, France.

[3] Becker, S.T., Bolte, H., Krapf, O., Seitz, H., Douglas, T., Sivananthan, S., Wiltfang, J., Sherry, E., Warnka, P.H. (2009). Endocultivation: 3D printed customized porous scaffolds for heterotopic bone induction, *Oral Oncology*, Vol. 45, No. 11, e181-e188, doi: 10.1016/j.oraloncology.2009.07.004.

[4] Greco, A., Licciulle, A., Maffezzoli, A. (2001). Stereolitography of ceramic suspensions, *Journal of Materials Science*, Vol. 36, 99-105, doi: 10.1023/A:1004899027360.

[5] Tan, K.H., Chua, C.K., Leon, K.F., Naing, M.W., Cheah, C.M. (2005). Fabrication and characterization of three-dimensional poly(ether-ether-ketone)/-hydroxyapatite biocomposite scaffolds using laser sintering, *Proceedings of the Institution of Mechanical Engineers*, Vol. 219, No. 3, 183-194, doi: 10.1243/095441105X9345.

[6] Nishikawa, M., Myoui, A., Ohgushi, H., Ikeushi, M., Tamai, N., Yshikawa, H. (2004). Bone tissue engineering using novel interconnected porous hydroxyapatite ceramics combined with marrow mesenchymal cells: quantitative and three dimensional image analysis, *Cell Transplant*, Vol. 13, No. 4, 367-376.

[7] Rose, F.R., Cyster, L.A., Grant, D.M., Scotchford, C.A., Howdle, S.M., Shakesheff, K.M. (2004). In vitro assessment of cell penetration into porous hydroxyapatite scaffolds with a central aligned channel, *Biomaterials*, Vol. 25, No. 24, 5507-5514, doi: 10.1016/j.biomaterials.2004.01.012.

[8] Allanic, A.-L., Schaeffer, J.-P. (2000). *Rapid prototyping process and apparatus*, Patent US6110409.

[9] Dormal, T. (2004). Industries et Technologies, juin 2004, n°859, 64-66.

[10] Charlier, T., Chaput, C., Doreau, F. (1997.) *Ceramic paste composition and prototyping method*, Patent WO0042471.

[11] Yukitoshi, K. (2000). *Resin composition for photofabrication of three dimensional objects*, Patent WO00/59972.
[12] Boilet, L., Descamps, M., Rguiti, E., Tricoteaux, A., Lu, J., Petit, F., Lardot, V., Cambier, F., Leriche, A. (2013). Processing and properties of transparent hydroxyapatite and β tricalcium phosphate obtained by HIP process, *Ceramic International*, Vol. 39, No. 1, 283-288.
[13] Seitz, H., Rieder, W., Irsen, S., Leukers, B., Tille, C. (2005). Three-dimensional printing of porous ceramic scaffolds for bone tissue engineering, *Journal of Biomedical Materials Research*, Vol. 74B, No. 2, doi: 10.1002/jbm.b.30291.
[14] Kundribskaja, S. (2010). Calcium orthophosphates as bioceramics: State of the art, *Journal of Functional Biomaterials*, Vol. 1, No. 1, 22-177, doi: 10.3390/jfb1010022.
[15] Clarinval, A.M., Boilet, L., Descamps, M., Leriche, A., Soyeur, Q., Wonnoye, D., Sforza, T., Hocquet,S., Lardot, V., Cambier, F. (2010). Synthèse de poudre phosphocalciques et mise en oevre par prototypage rapide, In: *Proceedings of Nantes Materiaux 2010 Symposium*, Nantes, France.
[16] Komlev, V.S., Mastrogiacomo, M., Pereira, R.C., Peyrin, F., Rustichelli, F., Cancedda, R. (2010). Biodegradation of porous calcium phosphate scaffolds in an ectopic bone formation model studied by X-ray computed microtomography, *European Cells and Materials*, Vol. 19, 136-146.
[17] Marchac, D., Greensmth, A. (2008). Long-term experience with methylmetacrylate cranioplasty in craniofacial surgery, *Journal of Plastic Reconstructive & Aesthetic Surgery*, Vol. 61, No. 7, 744-752, doi: 10.1016/j.bjps.2007.10.055.
[18] Vorndran, E., Klarner, M., Klammert, U., Grover, L.M., Patel, S., Barralet, J.E., Gbureck, U. (2008). 3D powder printing of β-tricalcium phosphate ceramics using different strategies, *Advanced Engineering Materials*, Vol. 10, No. 12, B67-B71, doi: 10.1002/adem.200800179.
[19] Tommasini, S.M., Nasser, P., Hu, B., Jespsen, K.J. (2008). Biological co-adaptation of morphological and composition traits contributes to mechanical functionality and skeletal fragility, *Journal of Bone and Mineral Research*, Vol. 23, No. 2, 236-246, doi: 10.1359/JBMR.071014.